PROCEEDINGS OF SPIE

SPIEDigitalLibrary.org/conference-proceedings-of-spie

# Organic semiconductor rubrene thin films deposited by pulsed laser evaporation of solidified solutions

N. Majewska
M. Gazda
R. Jendrzejewski
S. Majumdar
M. Sawczak
G. Śliwiński

SPIE.

# Organic semiconductor rubrene thin films deposited by pulsed laser evaporation of solidified solutions

N. Majewska[a*], M. Gazda[b], R. Jendrzejewski[a], S. Majumdar[c], M. Sawczak[a], G. Śliwiński[a]
[a] Department of Photophysics, Institute of Fluid-Flow Machinery, Polish Academy of Sciences, 14 Fiszera St, 80-231 Gdańsk, Poland
[b] Faculty of Applied Physics and Mathematics, Gdańsk University of Technology, 11/12 Narutowicza St. 80-233 Gdańsk, Poland
[c] Department of Physics and Astronomy, University of Turku, 20014 Turku, Finland

## ABSTRACT

Organic semiconductor rubrene ($C_{42}H_{28}$) belongs to most preferred spintronic materials because of the high charge carrier mobility up to 40 $cm^2(V{\cdot}s)^{-1}$. However, the fabrication of a defect-free, polycrystalline rubrene for spintronic applications represents a difficult task. We report preparation and properties of rubrene thin films deposited by pulsed laser evaporation of solidified solutions. Samples of rubrene dissolved in aromatic solvents toluene, xylene, dichloromethane and 1,1-dichloroethane (0.23-1% wt) were cooled to temperatures in the range of 16.5-163 K and served as targets. The target ablation was provided by a pulsed 1064 nm or 266 nm laser. For films of thickness up to 100 nm deposited on Si, glass and ITO glass substrates, the Raman and AFM data show presence of the mixed crystalline and amorphous rubrene phases. Agglomerates of rubrene crystals are revealed by SEM observation too, and presence of oxide/peroxide ($C_{42}H_{28}O_2$) in the films is concluded from matrix-assisted laser desorption/ionization time-of-flight spectroscopic analysis.

**Keywords:** rubrene organic semiconductor, spintronics, thin films, pulsed laser evaporation.

## 1. INTRODUCTION

Organic crystalline materials able to mediate or control a spin polarized electronic signal evoke much interest during last decade. These materials found application, alone or in conjunction with inorganic semiconductors, as the active layers in a variety of electronic devices, e.g. organic photovoltaic cells, light emitting diodes (OLEDs), lasers, sensors, and radio frequency identification tags (RFIDs) [1]. Also, the spintronic information storage based on the giant magnetoresistance effect (GMR) greatly contributed to the fast rise of data density stored in hard discs.Organic semiconductors possess remarkably long spin relaxation times, are mechanically flexible and can be easily structural modified, while showing a low carrier mobility compared to inorganic semiconductors as observed for other polycyclic aromatic hydrocarbons (acenes) such as tetracene ($C_{18}H_{12}$), pentacene ($C_{22}H_{14}$) and rubrene (tetraphenyltetracene, $C_{42}H_{28}$) [2-4]. The latter one has been widely applied ca three decades ago as a laser dye of excellent luminescence properties [5] . The reneval interest in rubrene is due to highest charge carrier mobility among organic semiconductor materials, in the range up to 20 - 40 $cm^2(V{\cdot}s)^{-1}$ [6]. The rubrene molecule is characterized by a size similar to other acenes (~ 1 nm) and consists of a tetracene backbone formed by four linearly fused benzene rings with a phenyl ring bonded on each side of the two central benzenes - see Fig. 1.

Similarly to other organic semiconductors the rubrene thin films can be fabricated by various growth techniques in either single crystal, polycrystalline or amorphous form. However, due to size limitation of devices based on single crystals and other practical issues such as cost-effective manufacturing of flexible devices the thin polycrystalline films are preferred from the point of view of industrial scale fabrication. While for growing of rubrene films different methods are reported such as growth from solutions and reprecipitation, and also physical vapor transport and thermal evaporation, the fabrication of a defect free, chemically clean, and good quality polycrystalline films for spintronic devices represents a challenge [8,9]. The literature shows that studies on this subject are performed also with use of the pulsed laser deposition (PLD) which is well proven in the stoichiometric growth of thin films of inorganic materials under controlled and

* natmaje1@gmail.com; phone: +48 58 5225313; fax: +48 58 3416144

Third International Conference on Applications of Optics and Photonics, edited by Manuel F. M. Costa,
Proc. of SPIE Vol. 10453, 104532H · © 2017 SPIE · CCC code: 0277-786X/17/$18 · doi: 10.1117/12.2276250

chemically clean conditions. However, only a few reports are published on the polymer, biomaterial and organic semiconductor (pentacene) thin films fabricated by this method [2,3,10]. The PLD growth of rubrene thin films and also systematic study of the structural, electronic, and magnetic properties of films grown on $La_{0.67}Sr_{0.33}MnO_3$ (LSMO) under optimized growth conditions were reported by us recently [11,12].

In frames of this work the rubrene layers are grown by means of the pulsed laser evaporation of rubrene solutions solidified at cryogenic temperatures. The laser pulses ablate small volumes of the frozen mixture (target) consisting of rubrene (guest) dissolved in organic solvent (matrix). This provide sufficient kinetic energy for transfer to and deposition of the organic molecules on substrate while the volatile molecules of the matrix are pumped away. This growth method is known as the matrix-assisted pulsed-laser evaporation and represents a modification of the versatile PLD technique dedicated for processing of sensitive materials of the organic and biological origin [13]. The literature shows that thin polymer and semiconductor films can be deposited in this way assuming the process conditions are properly selected which is not trivial [8]. The use of a target obtained by means of the discussed method for ablative production of colloidal rubrene nanoparticles in liquid has been reported, too [10].

Results reported here indicate that the applied method ensures an efficient growth of rubrene films if most of the laser energy is absorbed by the target matrix. This also minimizes degradation of the fragile organic guest molecules and allows for a better control of the film morphology. The content of crystalline phase is concluded from coincidence of the Raman spectra and the film structure obtained from the optical, AFM and SEM observations. Effects of the solvent, rubrene concentration, and laser irradiation conditions on the film growth are discussed.

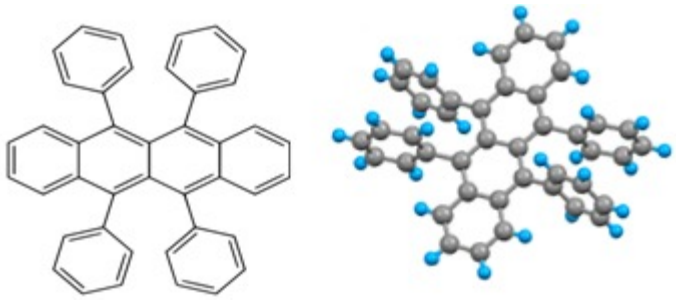

Figure 1. The chemical structure (left) and spatial conformation (right) of the rubrene molecule.

## 2. EXPERIMENTAL

For preparation of the target material selected solvents were analysed from the point of view of the rubrene solubility, tendency to concentration dependent sedimentation and recrystalisation at room temperature. The absorbance spectra of the solvents were measured and positions of the absorption bands in relation to available laser wavelengths of 266, 355, 532 and 1064 nm were taken into account - see Fig. 2. Finally, the organic aromatic solvents: toluene, xylene, dichloromethane (DCM) and 1,1-dichloroethane (DCA) were chosen due to the required match of laser irradiation with absorption bands of the solvents while minimizing the photodecomposition danger of the organic molecules. Solutions were prepared by dissolving of the commercially available rubrene powder (Sigma-Aldrich, purity 99,99%) in the solvents (analytical grade) under continuous stirring at concentrations up to the saturation level (< 1%) at room temperature until the liquid became uniform in color and transparency and the rubrene sedimentation was not observed.

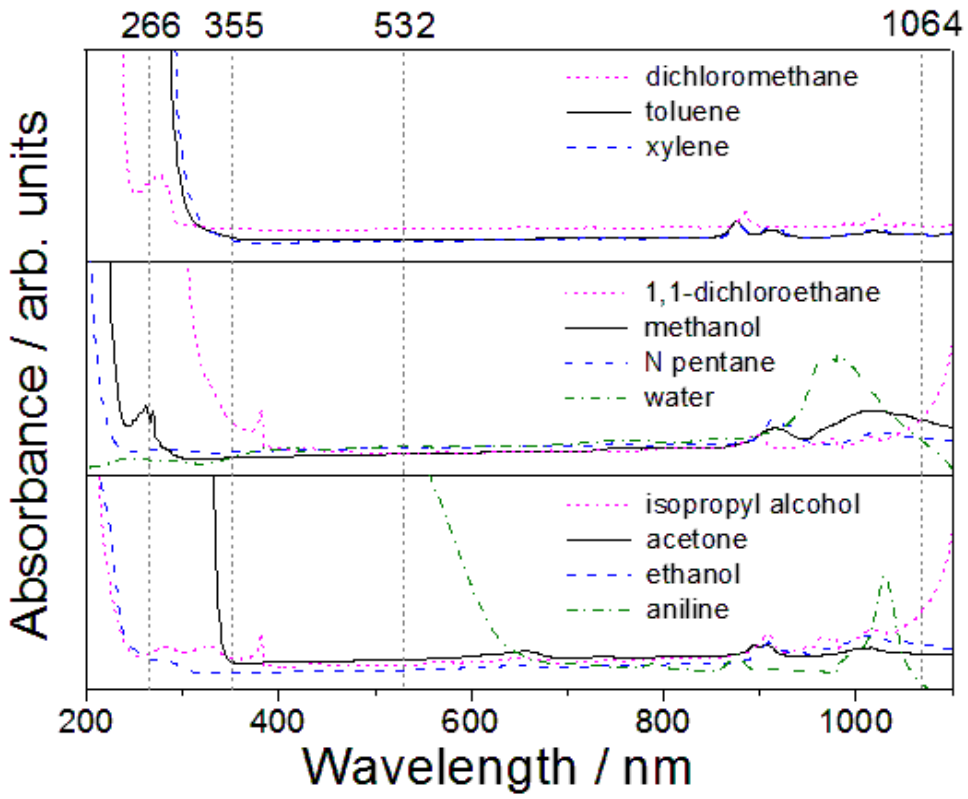


Figure 2. Absorbance spectra of selected solvents; the spectrum of water is given for comparison and the available laser emission wavelengths of 266, 355, 532 and 1064 nm are marked by vertical lines.

The solidification of liquid samples and deposition of the films were carried out in a vacuum chamber evacuated by a turbo-pumping stand and equipped with the closed-cycle He cryostat (Leybold) and substrate holder with heater and temperature sensor. For target preparation an amount of about 1 $cm^3$ of the rubrene solution has been injected into the sample reservoir located on the cold finger of the cryostat while controlling its temperature at a level slightly above the boiling point of the applied solvent and at pressure temporarily elevated above the backing value of $10^{-6}$ mbar. After liquid-solid phase transition of the solution both the chamber pressure and target temperature were decreased and continuously controlled for stable operation. The Si, glass or ITO/glass substrates (1 x 1 $cm^2$) sonicated for 15 minutes in deionized water and next in ethanol were mounted at a distance selected in the range of 3-4 cm from the target.

The ablation was provided by a pulsed (6 ns) 1064 nm or 266 nm laser (Quantel B) of the beam intensity and diameter controlled by a diaphragm and lens telescope in the optical path. An additional lens mounted on the motorized, numerically controlled XY stage ensured stepwise rastering of the target surface by the focused laser beam ( spot size of 210 ± 53 μm). This provided a roughly constant ablation conditions in a rectangular surface area of about (1 x 1,4) $cm^2$ of the target. A schematic view of the experimental setup is shown in Fig. 3. The applied laser fluence and pulse frequency were in the range of 0.22-10.37 J/$cm^2$ and 2-10 Hz, respectively. In dependence on the solvents the target temperatures were selected from the range of (16.5 - 165) K and also different substrate temperatures (293-423) K were applied during deposition, too. After deposition the samples were placed and stored in container filled with $N_2$ and kept in darkness, because of the rubrene chemical instability under daylight illumination in ambient air and the resulting formation of rubrene peroxide.

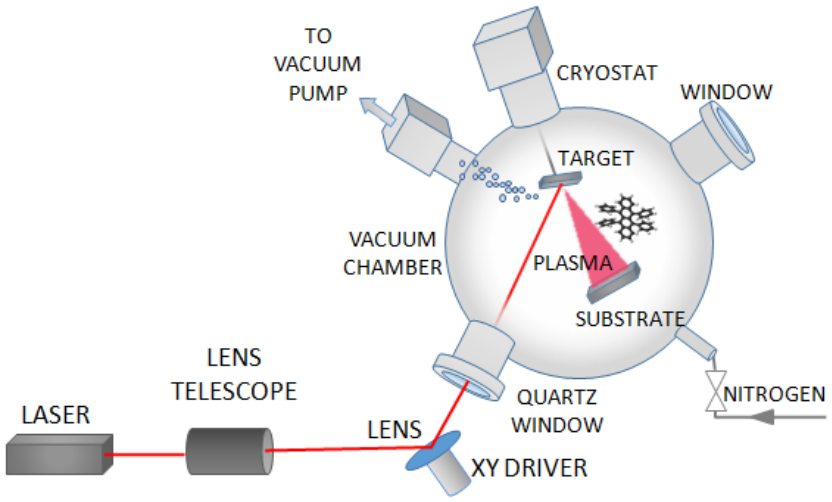


Figure 3. Scheme of the experimental setup.

The absorbance spectra of the deposited thin films and of rubrene powder and substrates for reference were recorded with use of the spectrophotometr Lambda 35 (Perkin Elmer). Raman measurements were performed by means of a confocal micro-Raman system InVia (Renishaw) operating with grating of 1200 groves/mm (resolution 1 $cm^{-1}$) and the lateral resolution on the sample surface was 5 μm. In order to minimize the rubrene luminescence the samples were excited at markedly reduced power of the 785 nm laser. For surface morphology observations the atomic force microscope (AFM) EasyScan (Nonosurf) operated with cantilever (Sicon W) in contact mode as well as the scanning electron microscope (SEM, Hitachi) with BSE detector were applied. The thickness and surface roughness of rubrene films were measured by means of the profilometer DektakXT (Bruker).

## 3. RESULTS

For thin film samples deposited by pulsed laser ablation of solidified rubrene solutions in xylene, DCM, DCE, toluene and DCE a nearly linear dependence was observed of the film thickness on the number of laser pulses applied at constant pulse repetition from the range of 2-20 Hz. Films of a thickness up to 100 nm were typically produced using 18 000 laser pulses at fluence above ablation threshold, i.e. from the range of 2-10.4 $J/cm^2$ depending on the solvent. Parameters characterizing the deposition experiments are summarized in Table 1.

In experiment where lower fluence values (< 1 $J/cm^2$) were applied the growth was not observed in case of toluene and DCE matrix. The experiments with use of the xylene and DCM matrices were unsuccessful most probably because of rubrene recrystalization in both cases. This was deduced from presence of sediment in the solutions already during its injection into the cooling reservoir. Depositions Despite careful selection of a relatively low rubrene concentration in xylene. For films deposited by ablation of the toluene/rubrene targets at 266 nm the photodecomposition of rubrene was observed in agreement with strong absorption bands in the UV region reported for rubrene [12]. These films revealed inhomogeneous amorphous structure with dominating presence of carbon despite various rubrene concentrations and relatively low laser fluences applied. In contrary, reproducible results were obtained with use of 1.1-DCE targets with rubrene at concentrations from the range of 0.5-0.7 %. and laser fluence of 4.1- 4.7 $J/cm^2$ and data of these samples are discussed in the following.

Table 1. The investigated solvents, rubrene concentrations and deposition parameters.

| Solvent | Melting temperature (K) | Rubrene concentration (%) | Irradiation wavelength (nm) | Laser fluence (J/cm$^2$) | Laser pulse Frequency (Hz) | Target Temp. (K) |
|---|---|---|---|---|---|---|
| xylene | 226 | 0.35 | 1064 | 10.37 | 2 | 17-65 |
| DCM | 176.5 | 0.23-0.97 | 1064 | 1.94-4.03 | 2-10 | 17-163 |
| 1,1-DCE | 176 | 0.50 | 1064 | 0.22-0.49 | 4-10 | 16.5 |
| toluene | 174 | ≤1 | 266 | 0.64-0.96 | 2 | 16.5 |
| 1,1-DCE | 176 | 0.70 | 1064 | 2.97-4.76 | 10 | 18-90 |

The microscope observation of the films produced from DCE-rubrene targets under the same conditions showed similar surface structure. Differences in roughness and distribution of larger surface irregularities have been ascribed to variations of the laser pulse energy and spot area during target scanning which both resulted in variation of the laser fluence estimated to ± 25%. The typically observed results (film sample #17 of 60) are summarized in Fig. 4. A clear evidence of the crystalline rubrene follows from comparison of the Raman spectra recorded in the range of 1000-1700 cm$^{-1}$ for several locations of the film surface (Fig. 4c) with that of the powder sample. Despite the relatively strong photoluminescence signal of rubrene the positions of most prominent bands corresponding to phenyl $A_g$ (1004 and 1303 cm$^{-1}$) and tetracene $B_g$ (1522 cm$^{-1}$) vibration modes are well resolved in most cases and agree with literature [10,12]. In contrary, bands around 1303 cm$^{-1}$ and 1606 cm$^{-1}$ which could indicate on presence of the amorphous phase are difficult to observe.

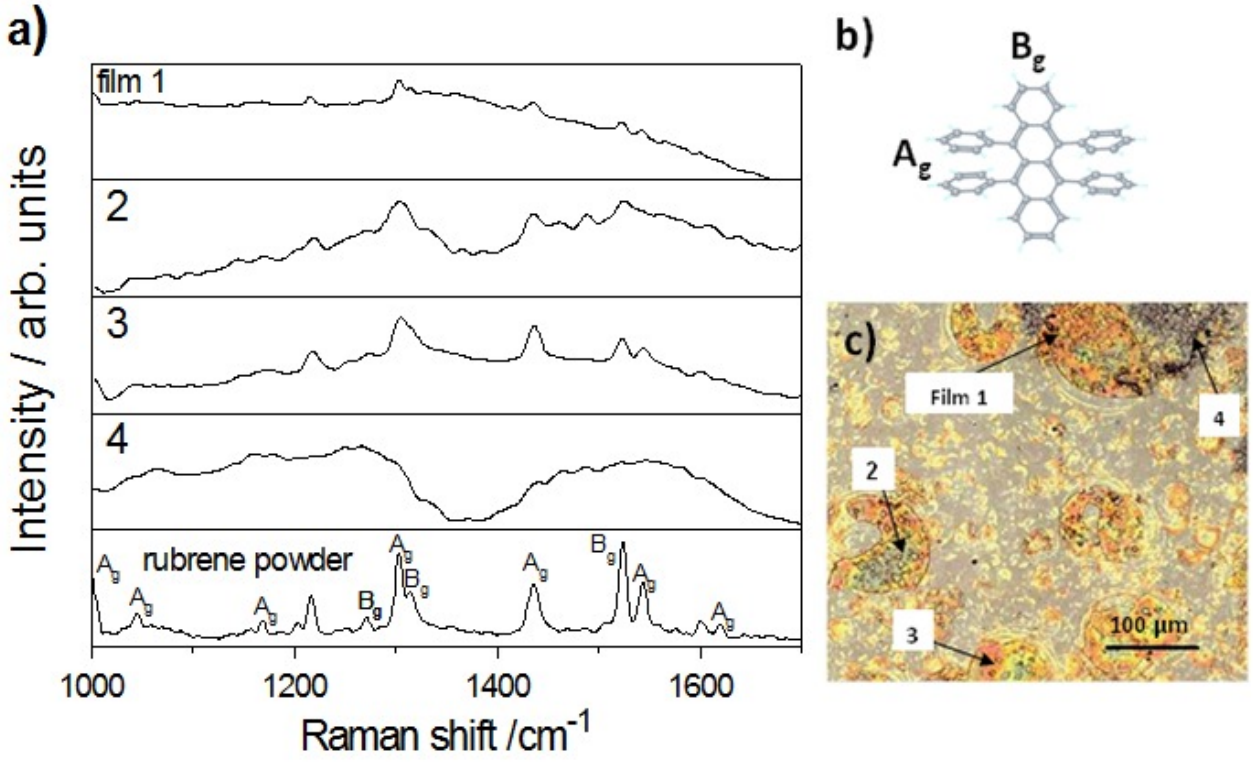


Figure 4. Raman spectra recorded for different areas of the rubrene film surface (sample # 16) and spectrum of the rubrene powder for reference (a), structure of the rubrene molecule and vibrational bands of tetracene core ($B_g$) and phenyls groups ($A_g$) (b), and locations of the Raman measurements, objective magnification x50 (c); the rubrene film was deposited with 18000 laser pulses at fluence of 4,06±1,02 J/cm$^2$ from 0.7% rubrene-DCE target (22 K) on glass substrate kept at room temperature.

The relation between the surface areas revealing concentrated bright spots and Raman band intensities recorded for these areas becomes more evident when a selected signal, e.g. characteristic for the crystalline rubrene is observed over extended area. This is shown by the linear scan of the Raman band intensity at 1003 $cm^{-1}$ ($A_g$ mode) recorded along a distance of 60 mm over the film surface in Fig. 5. Indeed, the recorded low intensities correspond to areas characterized by a low number of spots and also presence of film discontinuities cannot be excluded, while intensity peaks indicate film areas of the highest crystalline content.

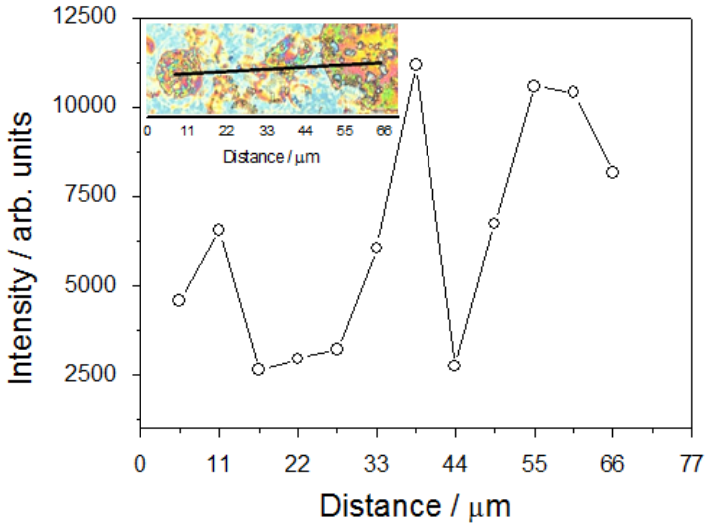


Figure 5. The line scan of Raman intensity excited at 785 nm and recorded at 1003 $cm^{-1}$ along a path of 60 μm on surface of the rubrene thin film grown on $Si/SiO_2$.

The surface morphologies observed in AFM and SEM images in Fig. 6 and obtained for rubrene thin films prepared from rubrene-DCE targets under various deposition conditions confirm in general the presence of crystalline and amorphous phases revealed by the Raman spectra.

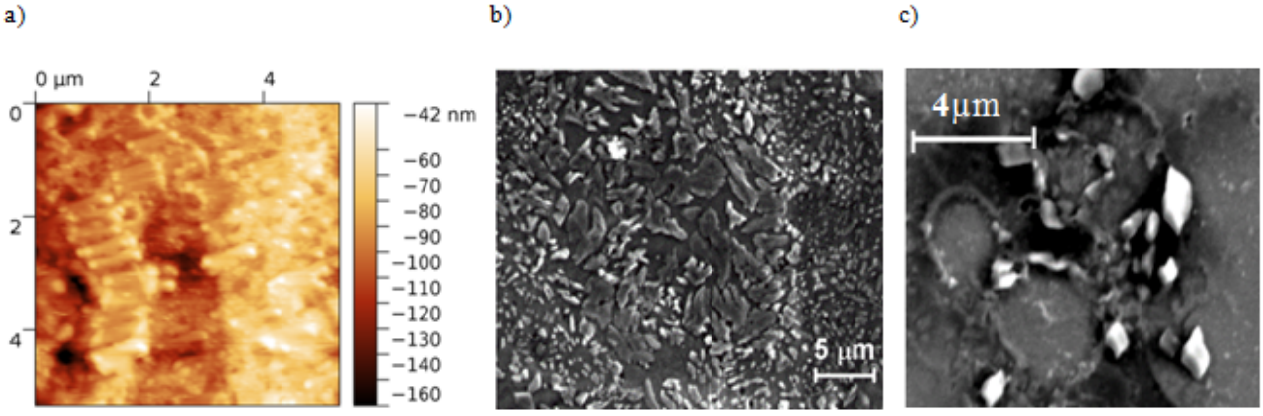


Fig. 6. Rubrene thin films of a thickness of 120 nm deposited from 0.5 % wt solution in 1.1-DCE on Si substrate using 18000 laser pulses at fluence of 3.6 $J/cm^2$; AFM scan showing presence of crystalline phase characterized by closely packed columnar structure (a), and SEM images showing crystallites embedded in the amorphous phase (b) and (c).

The typically observed crystallites are characterized by differences in the size, shape, and also in the orientation and degree of the dendritic growth. This depends on the deposition conditions and indicate that their optimal selection needs to be found in order to fabricate the homogeneous polycrystalline films with minimized content of the amorphous phase. An improvement of the preparation results can be considered by means of the RIR-MAPLE method based on use of emulsified target material being a mixture (emulsion) of organic material dissolved in appropriate solvent and water as proposed by Stiff-Roberts and coworkers [14]. This approach was intended for deposition of organic thin films with application potential in the production of heterojunction solar cells. Recent results obtained by the same group with use of this technique indicate that not only the organic thin film growth, but also the film structure (morphology, surface roughness) directly depend on composition of the emulsion [106]. It is also shown that the detrimental nanoscale aggregation and clustering of particles which is frequently observed for composite organic films fabricated by other techniques can be minimized in case of the emulsion-based approach by a sequential deposition with use of the multi-component, sectioned targets.

In case of the rubrene deposition considered here the already mentioned molecular conformation with phenyl rings twisted in respect to the tetracene backbone causes non-planarity of the molecule. This in turn hinders the growth of crystalline phase and and is the most probable reason of the observed undesirable growth effects such as amorphous films with spherullitic structures [15].

The absorbance spectra in UV-Vis spectral range from 400 to 700 nm obtained for rubrene films produced from targets of different rubrene contents are shown in Figure 7. In comparison to the reference data of rubrene powder (dashed line) the spectrum of sample 17 is similar regarding intensity but shows the well resolved characteristic $\pi - \pi^*$ band at 522 nm (2,37 eV) along with progression of vibronic bands associated with the C–C stretching of rubrene molecule.in agreement with literature [10]. These bands are slightly red shifted and also the overall intensity is much weaker in case of the film deposited from target of a lower rubrene content (sample 16). The effect can be associated with a different (or incomplete) coverage of the substrate in the latter case observed in microscope images (not shown) and to a lesser extend with difference in nucleation and film growth conditions for Si and glass substrates. However, for reliable results regarding this concentration effect the collecting of additional data is in progress.

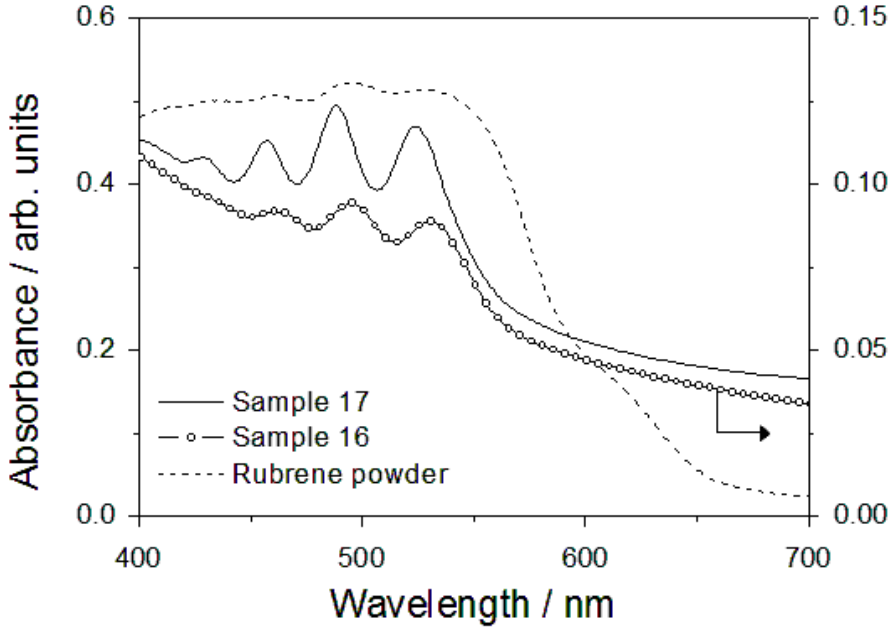


Fig. 7. Absorbance spectra of the 120 nm thick rubrene films on Si (solid line, sample #17) and on glass (split line, sample #16) deposited from 0.47% and 0.7 % wt solutions in 1,1-DCE, respectively; the spectrum of rubrene powder (dashed line) is given for reference.

In order to clarify the chemical composition of the amorphous phase observed in most of the produced samples the representative ones were analyzed by means of the matrix-assisted laser desorption/ionization time-of-flight (MALDI-TOF) mass spectroscopy. The obtained results indicated on prevailing presence of rubrene ($C_{42}H_{28}$) and also rubrene oxide/peroxide such as ($C_{42}H_{28}O_2$) [16].

It is worth mention too, that the post heating (annealing) applied for some samples at temperatures up to about 400 K did not resulted in structure changes which was concluded from the Raman spectra and microscope observations, in contrary to results reported for the phase transformation and growth of crystallites in case of the thermally evaporated rubrene. Nevertheless, the spectroscopic data and morphology observation of rubrene thin films fabricated in this work show a marked improvement regarding the film structure and content of the crystalline phase compared to films prepared by means of the PLD method reported previously [12].

## 4. CONCLUSION

We have demonstrated that thin films of the rubrene organic semiconductor can be fabricated using the pulsed laser evaporation of solidified solution. It has been found that among a variety of tested solvents the application of DCE and targets prepared from 1.1-DCE-rubrene solutions show satisfactory results in case of the 1064 nm laser applied for pulsed deposition. The spectroscopic data and structure observations of the obtained films indicate consistently on presence of agglomerates of rubrene crystals embedded in amorphous phase (rubrene oxide and peroxide). The content of crystalline phase and presence of characteristic vibronic bands in the absorption spectra of the films both confirm the general conclusion that the applied deposition method make possible the film growth and photodegradation of rubrene molecules can be controlled by selection of the process parameters. Research on this topic and the next step on preparation of the $SiO_2$/ITO/rubrene/Al device structures for measurements of the electronic and spin transport properties is in progress.

## ACKNOWLEDGMENTS

Authors acknowledge the inspiration and support of the Molspin Cost Action CA15128.

## REFERENCES

[1] Dediu, V., Hueso, L. E., Bergenti, I. and Taliani, C., “Spin routes in organic semiconductors”, Nature Mater. 8, 707-716 (2009).
[2] Blanchet, G. B.; Fincher, C. R. and Malajovich, I., “Electrogenerated chemiluminescence of aromatic hydrocarbon nanoparticles in an aqueous solution”, J. Appl. Phys. 94, 6181-6184 (2003).
[3] Salih, A. J.; Lau, S. P.; Marshall, J. M.; Maud, J. M.; Bowen, W. R.; Hilal, N.; Lovitt, R. W.; Williams, P. M “Improved Thin Films of Pentacene via Pulsed Laser Deposition at Elevated Substrate Temperatures”, Appl. Phys. Lett. 69, 2231-2233 (1996).
[4] Chrisey, D. B. and Hubler, G. K., “Laser Deposition of Polymer and Biomaterial Films”, Chem. Rev. 103, 553-576 (2003).
[5] Lehmannsroben, H., "Photophysical Properties and Laser Performance of Rubrene", Appl. Phys. B 1988, 47, 195.
[6] Hasegawa, T. and Takeya, “Organic field-effect transistors using single crystals”, J., Sci. Technol. Adv. Mater. 10, 024314 (2009).
[7] Podzorov, V., Pudalov, V. M. and Gershenson, M. E., “Field effect transistors on rubrene single crystals with parylene gate insulator”, Appl. Phys. Lett. 82, 1739 (2003).
[8] Zeng, X., Wang, L., Duan, L. and Qiu, Y., Homoepitaxy growth of well-ordered rubrene thin films”, Cryst. Growth Des. 8(5), 1617-1622 (2008).
[9] Omer, K. M. and Bard, A. J., “Electrogenerated chemiluminescence of aromatic hydrocarbon nanoparticles in an aqueous solution”, J. Phys. Chem. C, 113(27), 11575-11578 (2009).

[10] O'Malley S. M., Amin M., Borchert J., Jimenez R., Steiner M., Fitz-Gerald J. M., Bubb D. M., "Formation of rubrene nanocrystals by laser ablation in liquids utilizing MAPLE deposited thin films", Chem. Phys. Lett. 595-596, 171-174 (2014).
[11] Grochowska, K., Majumdar, S., Laukkanen, P., Majumdar, H. S., Sawczak, M., Śliwiński, G., "Pulsed Laser Deposition of Organic Semiconductor Rubrene Thin Films", Proc. SPIE, 94470F- 1−7 (2014).
[12] Majumdar, S., Grochowska, K., Sawczak, M., Śliwiński, G., Huhtinen, H., Dahl, J., Tuominen, M., Laukkanen, P., Majumdar, H. S., "Interfacial properties of organic semiconductor-inorganic magnetic oxide hybrid spintronic systems fabricated using pulsed laser deposition", ACS Applied Materials & Interfaces 7, 22228-22237 (2015).
[13] Piqué, A.,Wu, P., Ringeisen, B. R., Bubb, D. M., Melinger, J. S., "Processing of functional polymers and organic thin films by the matrix-assisted pulsed laser evaporation (MAPLE) technique", Appl. Phys. A, 105, 517 (2011).
[14] Ge, W., Atewologun, A., Stiff-Roberts, A., "Hybrid nanocomposite thin films deposited by emulsion-based resonant infrared matrix-assisted pulsed laser evaporation for photovoltaic applications", Organic Electronics, 22, 98–107, (2015).
[15] Kafer, D, Ruppel, L., Witte, G., Woll, C., Role of Molecular Conformations in Rubrene Thin Film Growth", Phys. Rev. Lett. 95, 166602 (2005).
[16] Huang, L., Liao Q., Shi Q., Fu H., Ma J., Yao J., " Rubrene micro-crystals from solution routes: their crystallography, morphology and optical properties", J. Mater. Chem. 20, 159-166 (2010).